A Numerical Analysis of Skin-PPE Interaction to Prevent Facial Tissue Injury

Rikeen D. Jobanputra (Rikeen.Jobanputra14@imperial.ac.uk)
Imperial College London
Jack Hayes
Imperial College London
Sravani Royyuru
Imperial College London
Marc A. Masen
Imperial College London

Research Article

Keywords: airborne matter, COVID-19 virus, PPE, micro-textures

Posted Date: May 20th, 2021

DOI: https://doi.org/10.21203/rs.3.rs-525768/v1

Version of Record: A version of this preprint was published at Scientific Reports on August 10th, 2021.
See the published version at https://doi.org/10.1038/s41598-021-95861-3.

A Numerical Analysis of Skin-PPE Interaction to Prevent Facial Tissue Injury.

Authors:

Rikeen D. Jobanputra[a], Jack Hayes[a], Sravani Royyuru[a], Marc A. Masen[a]

[a]Tribology Group, Department of Mechanical Engineering Imperial College London

Correspondence to Rikeen D. Jobanputra: Rikeen.Jobanputra14@imperial.ac.uk

Abstract

The use of close-fitting PPE is essential to prevent exposure to dispersed airborne matter, including the COVID-19 virus. The current pandemic has increased pressure on the healthcare system, leading to medical professionals using high-grade PPE for prolonged times, resulting in device-insduced skin injuries. This study focuses on computationally improving the interaction between skin and PPE to reduce the likelihood of discomfort and tissue damage. A finite element model is developed to simulate the movement of PPE against the face during day-to-day tasks. Due to limited available data on skin characteristics and how these vary interpersonally between sexes, races and ages, the main objective of this study was to establish the effects and trends that mask modifications have on the resulting subsurface strain energy density distribution in the skin. These modifications include the material, geometry and interfacial properties. Overall, the results show that skin injury can be reduced by using softer mask materials, whilst friction against the skin should be minimised, e.g. through use of micro-textures, humidity control and topical creams. Furthermore, the contact area between the mask and skin should be maximised, whilst the use of soft materials with incompressible behaviours (e.g. most elastomers) should be avoided.

Introduction

During the COVID-19 pandemic, healthcare professionals globally have been using personal protective equipment (PPE) for increased durations. The prolonged use of facial PPE, such as respirator masks, visors and face shields, may lead to the development of a range of skin issues, including irritation and injuries such as skin tears, pressure injuries and urticaria[1–6]. Respiratory protective equipment has been widely reported to cause skin reactions such as contact dermatitis, acne, facial itch and rash[7–9]. Lan et al report skin damage related to general protective measures occurring in up to 97% of health care workers, of which the nasal bridge has the highest prevalence[10]. Yen et al report that up to 71% of healthcare workers who wear PPE experience burning and itching sensations[11]. Discomfort and irritation may lead to the improper use of PPE, whilst skin injury might result in lost hours with medical and care staff being absent from work. In addition, a compromised skin barrier adds a potential entry route for COVID-19 infection[12]. Jiang et al correlated PPE-induced skin injury with heavy sweating, the use of higher-grades of PPE and the duration of continued use of PPE[13].

A key feature of tight-fitting or sealing PPE is that there is a close contact between the PPE and the skin, resulting in the skin being subjected to a combination of normal and shear forces. Manifestations of these loads acting on the skin range from indentation marks at the locations of PPE-skin contact to deep-tissue bruising across a larger area. Excessive loading of the skin can result in lesions at the skin surface, which can develop into erythema and mild irritations [12,14–16.] Various causative pathways to severe skin injuries have been presented in literature[17]. Loading of the skin may result in occlusion of the capillaries and restricted lymph flow, which will set off a cascade of biochemical processes. The resulting ischaemic response of the cell includes hypoxia, lack of nutrients and the build-up of metabolic waste products and will lead to a breakdown of cell organelles, triggering apoptosis or necrosis[9,18–20]. These effects at the cellular level, caused by applied external forces and local tissue deformation, result in macroscopic tissue injury at the sites of bony prominences, such as the nasal bridge, cheekbones and forehead [13 21].

It has long been established that shear forces acting on the skin result in damage occurring at significantly lower pressures than when only a normal load is applied [22–25] . In the contact between skin and PPE, three primary mechanisms can be identified that generate shear stresses at the skin interface. Firstly, static friction, sometimes also referred to as

'shear' or 'stiction', which prevents sliding of the PPE. Secondly, local relative motion between the PPE and skin, e.g. as a result of speaking when wearing PPE, causing rubbing of the PPE against the skin. Finally, upon the compression, the skin and PPE will deform perpendicular to the direction of loading by different amounts due to their respective Poisson's ratios, resulting the development of shear forces at the interface. [23–25]

Preventing PPE-related skin injury requires a better understanding of the interaction between the PPE and the skin, in addition to the effects of this interaction on the strains and stresses inside the tissue. Common treatments to alleviate friction-related injuries involve the application of hydrocolloid dressings [26,27] and the use of moisturisers. However, it was found that incorrect applications of moisturisers before and after PPE application may increase infection risk[28]. Previous investigations on PPE have mainly focussed on modelling the pressure that acts on the surface of the skin, with the objective of ensuring an appropriate seal and maintaining a level of user comfort[29–31]. However, the effects of PPE-skin interaction on the stresses and strains inside the tissue have not previously been investigated. Finite Element Analysis (FEA) is an efficient tool to model and visualise the local subsurface stress and strain levels within the tissue [32] and will be used to provide insight into the effects on the skin of interacting with PPE. [30,31] and the use of moisturisers.

The purpose of this investigation is to understand how the mechanical burden on the skin is affected by the characteristics of the PPE in terms of its material, geometric and interfacial properties. To enable this, the interaction between skin and a model respirator mask is examined using a parameterised finite element model. Following Oomens' work on tissue damage[33], the strain energy density (SED) in the skin was taken as the quantitative measure representing local tissue failure. A series of simulations enabled the quantification of the efficacy of the respirator mask alterations and its interaction with facial skin, in order to provide information on how to reduce skin injury amongst PPE wearers. A set of readily implementable guidelines regarding the use and design improvements of PPE will be defined based on the obtained results.

Results

The parametric study was conducted using FEA to investigate the effects of independently altering the mask material, and its geometric and interfacial properties. The mask is loaded against the skin with a load of 5 N and subsequently subjected to a lateral motion of 2 mm to represent the sliding and relative motion of tightened/fitted PPE during day-to-day tasks, thus inflicting shear stresses on the skin. The facial injuries observed in users of PPE are representative of a combination of deep-tissue injury, such as bruising and more superficial injuries, such as blistering and abrasion. Using a combination of in-vivo experiments and finite element modelling, Oomens[33] related the extent of localised tissue breakdown to the amount of deformation energy at that site. This metric was therefore adopted in the present study, recording the maximum SED in the dermis during contact with the mask. Material characteristics that were varied within the study were the stiffness E and the Poisson's ratio ν of the respirator mask. The geometric and interfacial properties altered in the investigation respectively include the contact length, L_c, representative of the contact area between the skin and PPE, and the adhesive friction coefficient, μ. Whilst the material and the geometry can be directly controlled by the designer, the friction in the contact is affected by a wide range of parameters, including the material being used and the surface microgeometry or texture, personal traits such perspiration and hairiness, as well as the application topical creams or lubricants. Table 1 lists the reference values used in this work, as well as the range of values investigated[29–31].

Table 1: The mask material, geometry and interfacial properties that were varied in this study.

Parameter	Reference Value	Variations in Study
Applied load [N]	5.0	-
Elastic modulus [kPa]	100	2 – 10,000
Poisson's ratio [-]	0.4	-0.2 – 0.49
Length of skin-PPE contact [mm]	4.0	3.0 – 4.8
Coefficient of friction [-]	0.5	0.1 – 1.1

Figure 1(a) displays the SED distribution in the dermis resulting from the contact with PPE for the reference mask indicated in Table 1. The SED distribution has a characteristic shape, with four main regions of interest:

- a sharp peak, P_L, in the upper dermis close to the skin surface, at the leading edge

- a sharp peak, P_T, in the upper dermis close to the skin surface, at the trailing edge,
- a larger region, A, of elevated SED values deeper into the tissue close to the boundary between the dermis and the hypodermis.

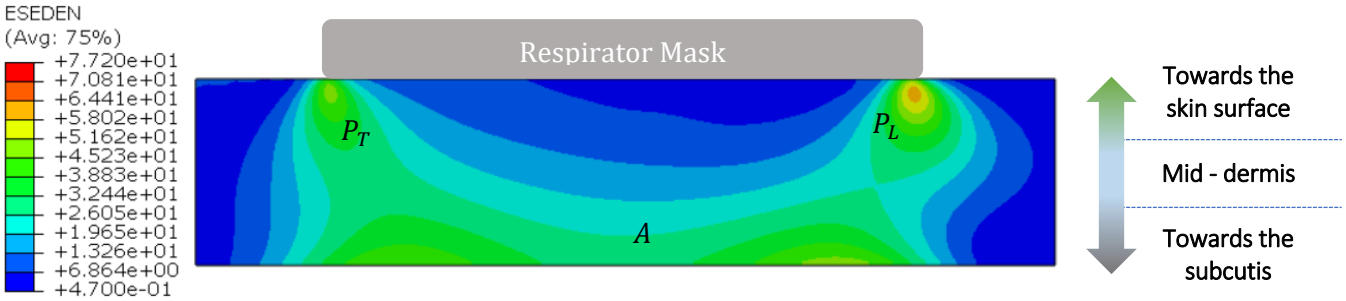

(a) The reference situation (E = 100 kPa, ν = 0.4, L_c = 4 mm and μ = 0.5) shows a SED distribution that has two characteristic peaks in the upper dermis near the skin surface, P_L at the leading edge and P_T at the trailing edge of the contact with the PPE. Due to the friction in the PPE-skin interface, the distribution is asymmetrical and the value for the SED at the leading edge is elevated compared to the trailing edge. The typical SED distribution also includes a large area of elevated SED deeper within the dermis, marked A, towards the subcutis.

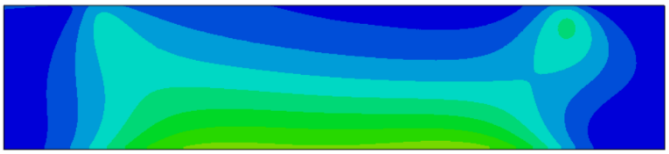

(b) When applying a compliant material (E = 5kPa) the SED reduces in the two peaks P_L and P_T, whilst deeper into the tissue, the SED appears elevated as marked by the larger area A.

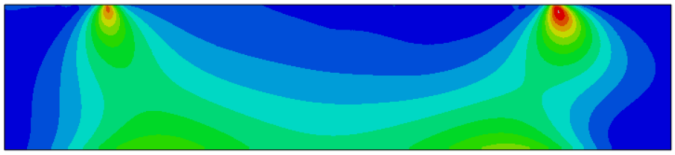

(c) For a stiff mask material (E = 5MPa), the SED at P_L and P_T is strongly increase, whilst being reduced towards the central deeper tissue A.

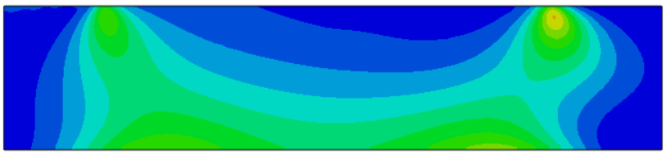

(d) A material with a Poisson's ratio ν= 0.1 results in a decreased SED in the upper dermisP_L, P_T with no substantial effect on the SED in the lower dermis A.

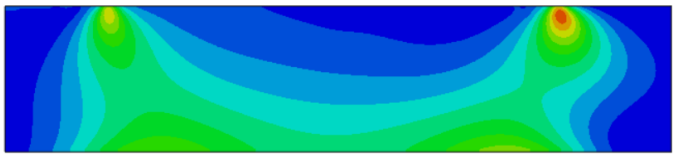

(e) A near incompressible material ν= 0.49 elevates SED at P_L and P_T. Whilst there is little effect on the SED in the lower dermis A, the SED in the region between P_L and A is elevated.

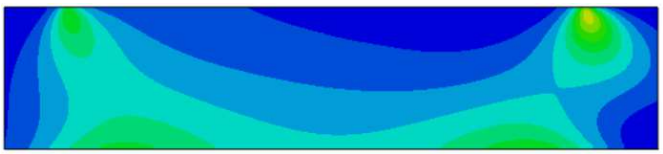

(f) When the load is distributed over a larger area of contact between the mask and the skin, in this case a contact length of 4.8 mm, the SED is distributed over a larger area and the SED is reduced throughout the skin.

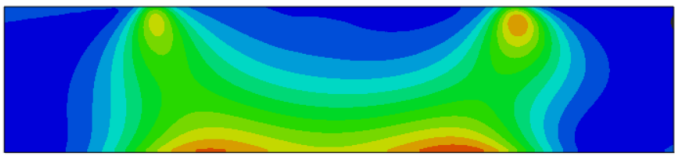

(g) For a smaller contact area, in this case a contact length of 3 mm, the SED is strongly increased, particularly deeper into the skin at region A. Compared to the reference situation, the increase at P_L and P_T is marginal.

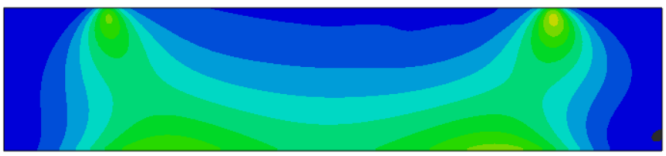

(h) Reducing the coefficient of friction (μ = 0.2) in the interface, reduces the SED values near the surface, particularly in P_L. The SED values between P_L and A increase slightly. No significant changes were observed for region A.

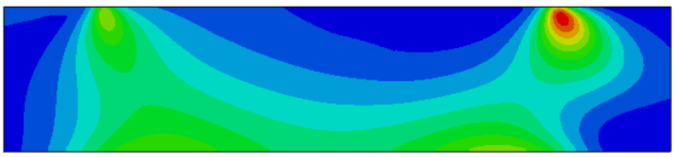

(i) Increasing the coefficient of friction (μ = 0.8) in the interface strongly increase SED at P_L. The effect deeper in the surface, in region A appears negligible. A minor decrease of SED values can be observed between P_L and A indicating a sharper, more isolated peak in P_L.

Figure 1: Distribution of the SED in the dermis as a result of using PPE. Red indicates an elevated value. Distribution displayed overlayed over the undeformed tissue.

Figures 1(b-i) illustrate the effects on the dermal SED distribution of varying the mask material, geometry and interfacial properties from the reference case. The various graphs show that increasing the stiffness of the material, the use of incompressible materials, and materials with a large coefficient of friction against skin all strongly increase

the SED values, but mainly near the skin surface. Reducing the area of contact between the respirator mask and the skin strongly increases the SED deeper in the skin. From these results it can be concluded that to reduce the SED in the skin requires investigating a combination of effects. In terms of the design of optimised PPE, the stiffness or modulus of the mask material is arguably the main design parameter. A wide range of materials are available for mask design, and the stiffness directly affects the contact area and contact pressure, as well as the friction in the skin-PPE interface. Therefore, the results obtained in this study will be presented as a function of the modulus of the mask material.

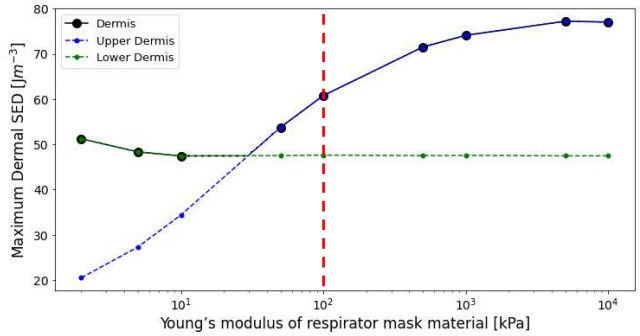

(a) With all other parameters held constant, stiffer mask materials result in the maximum dermal SED to be located in the upper dermis (blue). Below E ≈ 30 kPa the maximum SED occurs in the lower dermis and its value increases with reducing mask stiffness.

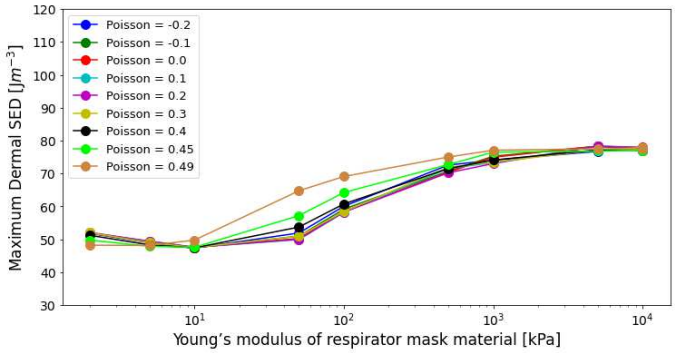

(b) Nearly incompressible materials (v → 0.5) with intermediate levels of stiffness (10 kPa < E < 1000 kPa) result in increases in maximum SED.

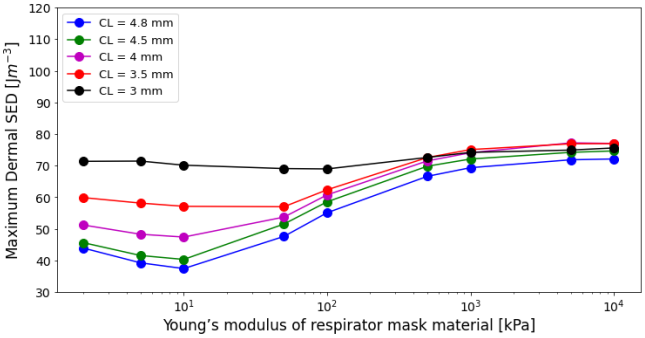

(c) A larger contact area between the skin and mask results in lower maximum SED values in the dermis. This effect is particularly pronounced for softer materials.

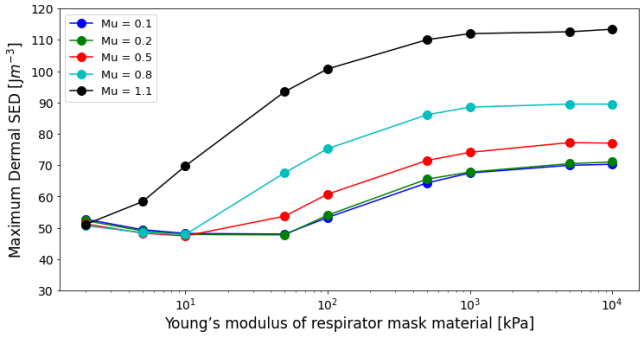

(d) For mask material stiffnesses above 10 kPa an increased interfacial friction coefficient results in substantially higher SED values in the upper dermis, particularly at the leading edge of the contact, P_L.

Figure 2: The effects of independently altering the mask properties on the maximum SED in the tissue. (a) Mask material stiffness, (b) Poisson's ratio, (b) area of contact, and (d) interfacial friction coefficient.

Stiffness of the mask material

The effect of altering the stiffness of the mask material is clearly visible in all four graphs in Figure 2, which show the evolution of the maximum dermal SED as a function of the stiffness of the mask material for a variety of cases. Taking Figure 2(a), which illustrates changes to the stiffness of the reference masks stiffness, the maximum SED in the skin increases following an S-shaped trend with increasing mask material stiffness. In general, a reduction of the mask stiffness leads to reduced maximum dermal SED in the upper dermis, as represented by the blue coloured curve. The SED in the lower dermis is not sensitive to the stiffness of the mask material, except for highly compliant materials, $E < 10\ \mathrm{kPa}$, which result in a slight increase in SED (green curve in Fig. 2a). Fig. 2(b-d)), show that the SED appears have a minimum level for compliant mask materials ($E \leq 50\ \mathrm{kPa}$), whilst the SED plateaus at a maximum value for stiff mask materials with $E \geq 10^3\ \mathrm{kPa}$.

Poisson's ratio

The Poisson's ratio describes the extent of deformation of a material perpendicular to the direction of loading, in this case the deformation of the mask material parallel to the skin surface when compressed against the skin. If the resulting deformation of the material is different than the deformation of the skin, an additional shear component is introduced in the interface. Therefore, the Poisson's ratio of the mask material is a potentially interesting parameter to take into

account during the design phase of respirators. Figure 2(b) illustrates that in general the effect of changing the Poisson's ratio on the SED in the skin is small and may be ignored. However, for mask materials with an intermediate stiffness $(10\ kPa < E < 500\ kPa)$ the near incompressibility of rubber materials ($\nu = 0.49$) may result in an increase of the SED. For example, for a mask with a Young's modulus of 50 kPa, this increase is more than 20%, from $\Xi = 53.7\ \mathrm{J\ m^{-3}}$ when $\nu = 0.40$ to $\Xi = 64.8\ \mathrm{J\ m^{-3}}$ when $\nu = 0.49$.

Size of the contact interface

Figure 2(c) shows that an increase of the contact area between the skin and the PPE results in decreased maximum SED values. For very soft materials this effect is quite pronounced; for $E = 10\ \mathrm{kPa}$ the maximum SED reduces 47%, from $\Xi = 70.1\ \mathrm{J\ m^{-3}}$ for a contact length $L = 3\ \mathrm{mm}$, to $\Xi = 37.5\ \mathrm{J\ m^{-3}}$ for a contact length $L = 4.8\ \mathrm{mm}$. For stiff mask materials ($E > 500\ \mathrm{kPa}$) the SED and approach a value of about $\Xi \sim 70\ \mathrm{J\ m^{-3}}$, irrespective of the contact length. For very small contact sizes ($L \sim 3\ \mathrm{mm}$) the maximum value of the SED in the skin appears to be relatively insensitive to the stiffness of the mask material, with the curve being nearly horizontal. It was found that increases in contact significantly reduced SED values in region A, whilst having a much smaller effect on the upper dermis (Fig. 3).

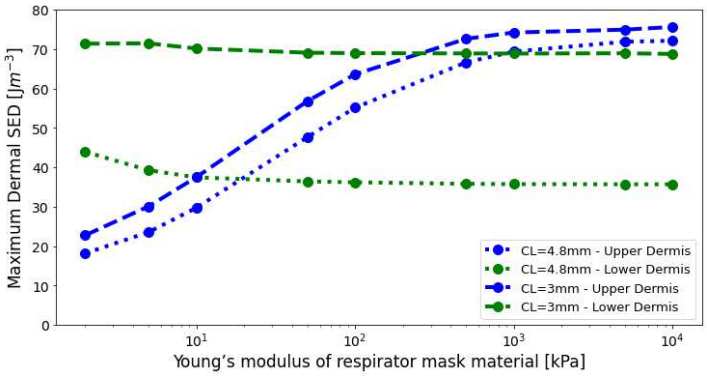

Figure 3: Evolution of SED in the tissue as a function of mask material modulus for contact lengths of 4.8 mm and 3 mm. Changes in contact length had a substantial effect on maximum SED in the lower dermis compared to the upper dermis.

Coefficient of friction in the skin-PPE interface

Figure 2(d) summarises the effects of the interfacial friction on the SED in the skin. The coefficient of friction has a large effect on maximum dermal SED, compare figures 1(h) and (j) which represent μ = 0.2 and 0.8, respectively. Elevated friction increases the maximum SED in the upper dermis, particularly at location P_L, with little to no effect on the values in the lower dermis. At elevated levels of friction, the value of the SED increases more with increasing friction. Overall, lower friction values can lead to a strong reduction of the SED in the dermis. There appears to be a minimum friction level of approximately $\mu = 0.2$, where a further reduction does not substantially maximum dermal SED.

Discussion

The presented results provide a general overview of the relationships between the characteristics of the respirator masks and the resulting burden on the skin as quantified using SED. The dermal SED distributions provide some insights into the underlying tissue damage mechanisms, and thus can be used to develop PPE design guidelines to reduce the likelihood of dermal injury. With this in mind, it is worth noting that whilst in this work the SED was used as the indicator for tissue damage and has been related to the onset of tissue injury under sustained loading[33], similar trends were obtained when analysing engineering parameters such as shear stress and deviatoric stress.

Limiting the stressing of the skin

Figure 1 displays a range of dermal SED distributions in the skin as a result of combined compression and translation of the mask against the face. Elevated SED values in the upper dermis towards the skin surface may indicate an increased risk of superficial skin injury, such as abrasions, surface rupture and tearing as well as delamination of the dermal-epidermal junction. Elevated values of the SED deeper in the skin may indicate an increased likelihood of deep tissue injuries such as bruising, full skin rupture and delamination of the skin from the underlying tissue.

Contact Area

The effect the area of contact between the PPE and the skin is clearly visible when comparing figures 1(a), (f) and (g). Reducing the contact area means the load is distributed over a smaller area, meaning the SED is strongly increased

throughout the skin, and particularly deeper in the skin at the region marked *A* (Figs 1g & 3). These results illustrate the importance of distributing the loads over a larger area, and thus the risk of pressure related injuries.

Stiffness

Materials with a reduced Young's modulus, often referred to as 'softer' materials, deform more under the same load than stiffer materials. As a result, the area of contact between the PPE and the skin increases and the strapping force of the PPE is distributed over a larger area. This supports the convention of softer materials being used in PPE with the aim of reducing discomfort and preventing injury. An additional effect of the increased area of contact between skin and PPE is that the maximum shear stress moves deeper into the tissue[34]. In Figure 2(a) it can be seen that reducing the stiffness of the PPE from 10 kPa to 2 kPa results in a modest but noticeable increase of the SED in the skin, driven by the lower dermis. When the stiffness of the mask material is larger than 1 MPa, i.e. significantly stiffer than the dermis, it was found that the maximum SED in the dermis did not vary significantly with further increasing stiffness. In that case the contact behaviour is dominated by the deformation of the skin whilst the PPE does not significantly deform.

Poisson's ratio

The Poisson's ratio of the mask material quantifies the extent to which the material displays the Poisson effect, i.e. its deformation in lateral direction following compression of the mask material against the skin. The Poisson's ratio for most engineering materials is about $\nu = 0.3$, whilst most rubbers are near incompressible with a value of $\nu \to 0.50$. Some cork materials do not display Poisson's effect-like behaviour and thus have $\nu = 0$. Theoretically, values for the Poisson's ratio range from $-1 < \nu < 0.50$. If the lateral deformation is different from the lateral deformation of the skin, a shear stress may be generated in the interface. The results indicate that the SED is relatively insensitive to this phenomenon, except for the specific combination of the mask comprising a material with intermediate stiffness ($10\ \mathrm{kPa} < E < 500\ \mathrm{kPa}$) and near incompressible behaviour ($\nu = 0.49$). Stiffer materials will only show a small deformation under loading, meaning that even for high values of ν the low strain of the mask material will not exert a substantial stress onto the skin surface. For highly compliant materials this effect is also minimal; whilst in this case the strains may be large, the modulus is low and therefore the resulting stress introduced into the interface will be too low to substantially affect the SED in the skin. These results, however, illustrate a potential issue for the typical softer materials used in respirator masks, which are often rubbery materials with a Young's modulus that falls in the "intermediate" range. This means that the use of these materials in PPE may possibly need further consideration.

Friction in the interface

A high interfacial friction coefficient between mask and skin results in increased levels of SED close to the skin surface. This is in agreement with literature, where high friction has been related to the development of superficial tissue injury[6,17,33], whilst deep tissue injury appears related to the direct application of pressure. In addition, friction may cause delamination of the dermal-epidermal junction, resulting in blisters and skin tearing [35–38]. Therefore, reducing the level of friction should be of primary concern when designing respirator masks. It is worth noting that friction in the skin-PPE interface is not a parameter that can easily be designed or optimised. The overall friction between the skin and PPE is a system parameter that depends on the mask material, the characteristics of the skin, as well as the loading and interfacial conditions. However, the literature mentions various ways to reduce friction, including the use of custom surface microgeometry or textures on the respirator masks, controlling the moisture in the contact and the use of specialised lubricants[2,39,40]. The application of a (micro-)texture to the surface of a device may be an effective measure to reduce the shear forces [41,42]. However, this may interfere with the sealing capability of the respirator.

Following mask usage, moisture levels in the skin are reported to increase [43]. The frictional response of skin is strongly dependent on humidity [44–46] and a moist environment macerates the skin and locally disrupts the skin barrier function [16,47]. Therefore, moisture control is an effective means of reducing friction and preventing injury. Breathable materials could be utilised, and inspiration may be drawn from the materials used in diapers and sanitary towels[48], both of which make contact with skin for extended periods of time in warm, humid conditions. An additional solution that may be considered, particularly by users that suffer from high friction or 'sticky' skin, is the use of a topical creams to alleviate the shear stresses in the skin-PPE interface[39,40].

Design Considerations

The results presented provide insight into the relative importance of the various investigated parameters. These results can be used to extract design guidelines for facial PPE. Figure 4 shows the potential reduction in skin loading resulting from the use of alternative geometrical, interfacial and material parameters, taking a silicone-based face mask as the

starting point[49,50]. The results confirm that interfacial and material alterations have a substantial effect on skin loading near the surface, whilst geometric alterations mainly effected the subsurface response.

Figure 4 also presents results obtained for an improved PPE, comprising an alternative material with increased contact area and reduced friction. The SED levels in the upper dermis reduce for every single alteration, resulting in an overall reduction of 46.6% for the improved model. The SED levels deeper in the tissue can only be reduced by changing the geometry of the mask. This enables the targeted augmentation of PPE to reduce the likelihood of injuries at specific dermal locations, deep tissue injury requires geometrical changes, whilst superficial injury may be alleviated through interfacial and material interventions.

Model/Parameter	E [kPa]	ν [-]	L_C [mm]	μ [-]
Silicone	210	0.49	4	0.6
Geometry altered	210	0.49	4.8	0.6
Interface altered	210	0.49	4	0.2
Materials altered	50	0.4	4	0.6
Improved PPE	50	0.4	4.8	0.2

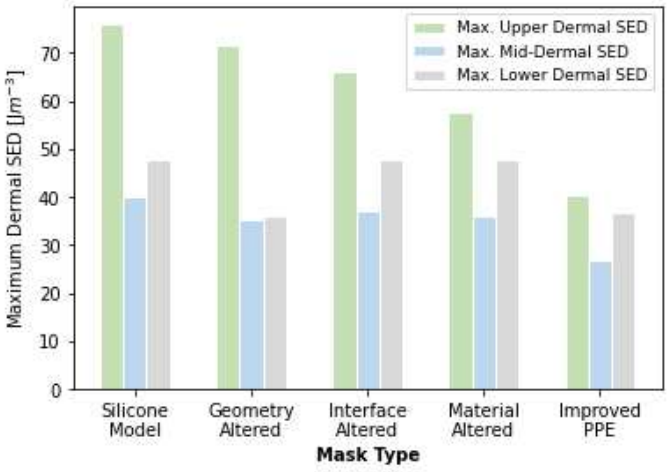

Figure 4: Table (left) showing different mask modifications compared to a silicone-based model. Graph (right) showing the SED in the upper (green), middle (blue) and lower dermis (grey) in response to the modifications.

Elastomeric materials are often used in respirator masks as the contacting layer against the skin. The low modulus of these materials distributes the pressure over a larger area, providing a degree of comfort whilst permitting a tight seal to form around the face to prevent leakage and viral exposure. However, the combination of the stiffness ($E < 1\ MPa$) and near incompressibility ($\nu \to 0.5$) of these materials may result in an elevated SED in the skin, as shown in Figure 2(b). More significantly, in contact against skin, elastomers exhibit friction coefficients that exceed 1[39,40,51] which significantly elevates dermal SED values. In terms of defining an optimal material to be used for facial PPE, the three parameters to consider are

- a modulus of about 100 kPa. Elastomers with a lower modulus would be beneficial from a pressure point of view, but are well known for their adhesive behaviour, which would elevate shear stresses in the skin
- non-incompressible behaviour ($\nu < 0.45$), to reduce compression-induced shear stress
- a coefficient of friction against skin of approximately 0.2, but definitely not exceeding 0.5

Whilst a single material with these properties may not be available, such a combination of characteristics may be achieved by using a soft, compressible inner layer (such as polymer foams or gels) covered with a thin, low-friction, breathable outer layer. Such a solution would confer beneficial bulk and interfacial properties to the user, reducing the risk of discomfort and injury.

Strengths and limitations to the study

The objective of the developed model was to record the strain energy density in the dermis when in contact with PPE with a variety of properties, in order to indicate the propensity for tissue failure. The accuracy of the obtained results depends on how representative the model and input parameters are. Whilst geometric data is available for facial tissue, there is a lack of data accurately describing its topology and mechanical properties. The mechanical properties of facial skin as reported in literature[52] and used in this model are linearly elastic, whilst this is sufficient for the purposes of this study, any further optimisation will require a better understanding of the nonlinearity and time-dependent behaviour of each layer of the skin. Additionally, the properties of facial tissues and craniofacial dimensions differ significantly between ages, ethnicities and sexes[53,54] and therefore further work is required to enable differentiation and optimization of PPE design for different demographics in order to ensure functionality and fitting whilst preventing injury and viral exposure[55]. Finally, damage thresholds for skin have not yet been established and these would provide useful insight into the likelihood of failure at different facial locations.

Materials & Methods

Simulating and Varying Skin-PPE Contact

Figure 5 shows a schematic diagram of the developed finite element model which comprises the contact between a respirator mask and facial skin tissue. A two-dimensional, isotropic finite element models was developed using ABAQUS CAE 2019. The mask model was compressed with a uniform pressure of 1000 N/m along the 5 mm long upper surface in order to indent the skin and generate a surface pressure with a magnitude similar to those found in literature[29,56,57]. The mask model was then translated by 2 mm to represent the relative motion of facial PPE whilst executing day-to-day tasks. As the exact damage threshold for skin has not been established and will vary interpersonally, the main purpose of this numerical investigation is to establish the effects and trends that a range of mask modifications have on the resulting subsurface SED distribution in the skin tissue, rather than attempting to obtain absolute values. The obtained results enable the recommendation of a range of potential mask modifications and help identifying the likely sites of skin failure.

Skin Model Development

The skin model consists of three layers, the epidermis, dermis and hypodermis or subcutaneous tissue, which were modelled as a continuum with flat interfaces between them. The model was developed as a single geometry before being partitioned into individual sections with different thicknesses and assigned material properties, thus simulating perfect adhesion between the skin layers. The skin comprises an epidermal layer with a thickness of 0.05 mm on top of a 1.3 mm thick dermal layer. This system is supported by a 1 mm subcutaneous tissue layer that provides a compliant boundary condition for the dermis by representing underlying tissue. The modelled section of skin has a width of 15 mm, of which a 6 mm wide section is designated as the dermal analysis site. The additional width of the skin model will mitigate any edge effects on the dermal analysis site and allows sufficient room at the surface for translation of the PPE. The skin model comprised 40014 quadratic plane strain elements and was given material and geometric properties from literature,[58–60] listed in Table 2. Data on facial skin was used where available, complemented with properties of volar forearm skin, as research suggests there is no significant difference in thicknesses, stiffness, Poisson's ratios and frictional behaviour[61,62].

Table 2: Material and geometric parameters of the simulated skin model.

Skin Layer	E [kPa]	ν [-]	Thickness [mm]
Epidermis	1500	0.48	0.05
Dermis	20	0.48	1.3
Hypodermis/Subcutis	2	0.48	1.0

In order to keep the skin taut, a pretensioning horizontal displacement of 0.1 mm was applied as a boundary condition on the left and right side of the model, whilst the base of the subcutis was restricted from vertical and rotational motion. Literature suggests adhesive friction is the main cause of macroscopic friction for unlubricated skin contacts[63]. Therefore, the surfaces were kept geometrically smooth and deformation friction on the microscale was ignored, whilst an interfacial coefficient of friction of 0.5 was applied between the mask and skin models. Following the translation of the skin, data was extracted from the dermal analysis site, underneath the mask-skin contact area. To reduce mesh effects, the reported maximum SED value is the average of the five elements with the highest SED values. Values are reported for the total skin, but also partitioned into an upper dermal segment (UD) and a mid-dermal segment (MD) both with a thickness of 0.4mm and a lower dermal segment (LD) of 0.5 mm. These dimensions were chosen purely for analysis purposes and to provide insight, and do not refer to any specific anatomical dermal sublayers.

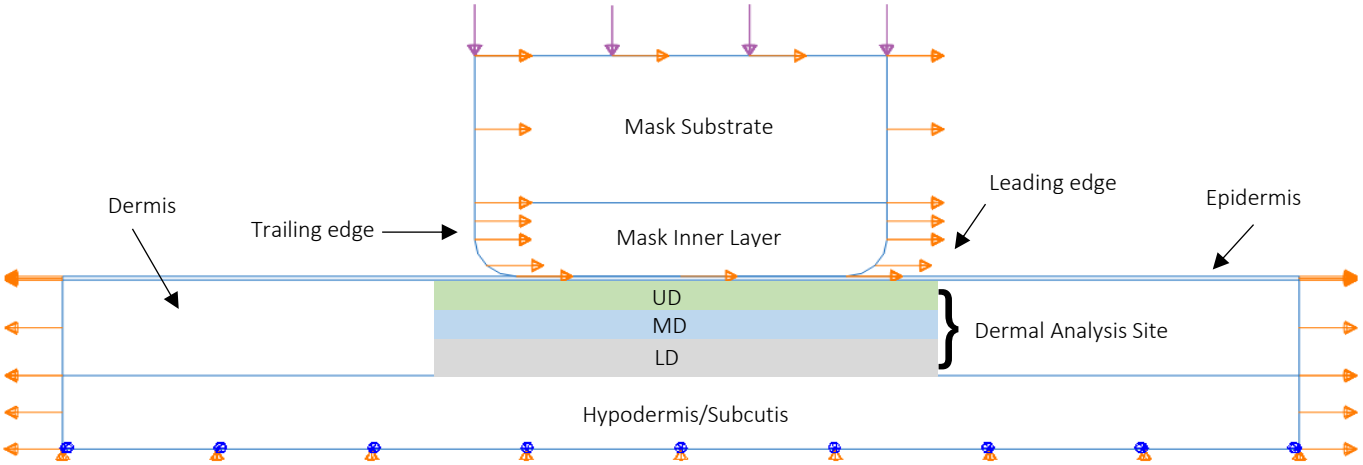

Figure 5: Schematic diagram detailing the compression and translation of a mask model against a skin model, in order to simulate PPE- Skin contact.

Mask Model Development

The mask model represents the edge or rim of a respirator mask which is in contact with the skin along the nasion, cheek and/or lower chin. The mask comprises two components, a 2 mm thick substrate which is exposed to the environment, and an inner layer which is in contact with skin and for which the properties are varied in this study. The total width of the mask is 5 mm and the substrate material is modelled with an elastic modulus of 7 MPa and a Poisson's ratio of 0.4. The inner layer of the mask is perfectly adhered to this substrate and has a thickness of 1 mm. The edges were given a radius of curvature of 0.5 mm, which was varied later in the study to adjust the area of contact between the skin and the PPE. The mask model was given a coarser mesh than the skin, consisting of 971 quadratic plane strain elements.

Acknowledgements

The authors wish to thank the Imperial College COVID-19 Response Fund for their financial support of this project.

Author Contributions

- R.D.J. - Preliminary Research, Methodology, Investigation, Writing (Original Draft + Review & Editing)
- J.H - Preliminary Research, Writing (Review & Editing)
- S.R. - Preliminary Research, Writing (Review & Editing)
- M.A.M. - Funding Acquisition, Supervision, Project Administration, Methodology, Writing (Original Draft + Review & Editing)

References

1. Zhou N-Y, Yang L, Dong L-Y, et al. Prevention and Treatment of Skin Damage Caused by Personal Protective Equipment: Experience of the First-Line Clinicians Treating SARS-CoV-2 Infection. *International Journal of Dermatology and Venereology*. 2020;3(2). doi:10.1097/JD9.0000000000000085

2. Gefen A. Skin Tears, Medical Face Masks, and Coronavirus. *Wound management and prevention*. 2020;66(4).

3. Zulkowski K. Understanding Moisture-Associated Skin Damage, Medical Adhesive-Related Skin Injuries, and Skin Tears. *Advances in Skin & Wound Care*. 2017;30(8). doi:10.1097/01.ASW.0000521048.64537.6e

4. Payne A. Covid-19: skin damage with prolonged wear of FFP3 masks. *BMJ*. Published online May 4, 2020. doi:10.1136/bmj.m1743

5. Dhandapani M, Jose S, Cyriac MC. Health Problems and Skin Damages Caused by Personal Protective Equipment: Experience of Frontline Nurses Caring for Critical COVID-19 Patients in Intensive Care Units. *Indian Journal of Critical Care Medicine*. 2021;25(2). doi:10.5005/jp-journals-10071-23713

6. Woo KY, Beeckman D, Chakravarthy D. Management of Moisture-Associated Skin Damage. *Advances in Skin & Wound Care*. 2017;30(11). doi:10.1097/01.ASW.0000525627.54569.da

7. Donovan J, Kudla I, Holness LD, Skotnicki-Grant S, Nethercott JR. Skin Reactions Following Use of N95 Facial Masks. *Dermatitis*. 2007;18(2). doi:10.1097/01206501-200706000-00013

8. al Badri F. Surgical mask contact dermatitis and epidemiology of contact dermatitis in healthcare workers. *Current Allergy and Clinical Immunology*. 2017;30(3):183-188.

9. Donovan J, Skotnicki-Grant S. Allergic Contact Dermatitis from Formaldehyde Textile Resins in Surgical Uniforms and Nonwoven Textile Masks. *Dermatitis*. 2007;18(1). doi:10.2310/6620.2007.05003

10. Lan J, Song Z, Miao X, et al. Skin damage among health care workers managing coronavirus disease-2019. *Journal of the American Academy of Dermatology*. 2020;82(5). doi:10.1016/j.jaad.2020.03.014

11. Yan Y, Chen H, Chen L, et al. Consensus of Chinese experts on protection of skin and mucous membrane barrier for health-care workers fighting against coronavirus disease 2019. *Dermatologic Therapy*. 2020;33(4). doi:10.1111/dth.13310

12. Sernicola A, Chello C, Cerbelli E, et al. Treatment of nasal bridge ulceration related to protective measures for the <scp>COVID</scp> -19 epidemic. *International Wound Journal*. 2020;17(5). doi:10.1111/iwj.13397

13. Jiang Q, Song S, Zhou J, et al. The Prevalence, Characteristics, and Prevention Status of Skin Injury Caused by Personal Protective Equipment Among Medical Staff in Fighting COVID-19: A Multicenter, Cross-Sectional Study. *Advances in Wound Care*. 2020;9(7). doi:10.1089/wound.2020.1212

14. Thorfinn J, Sjöberg F, Lidman D. Sitting can cause ischaemia in the subcutaneous tissue of the buttocks, which implicates multilayer tissue damage in the development of pressure ulcers. *Scandinavian Journal of Plastic and Reconstructive Surgery and Hand Surgery*. 2009;43(2). doi:10.1080/02844310902749455

15. Loerakker S, Stekelenburg A, Strijkers GJ, et al. Temporal Effects of Mechanical Loading on Deformation-Induced Damage in Skeletal Muscle Tissue. *Annals of Biomedical Engineering*. 2010;38(8). doi:10.1007/s10439-010-0002-x

16. Hua W, Zuo Y, Wan R, et al. Short-term skin reactions following use of <scp>N95</scp> respirators and medical masks. *Contact Dermatitis*. 2020;83(2). doi:10.1111/cod.13601

17. Bouten C v., Oomens CW, Baaijens FP, Bader DL. The etiology of pressure ulcers: Skin deep or muscle bound? *Archives of Physical Medicine and Rehabilitation*. 2003;84(4). doi:10.1053/apmr.2003.50038

18. Mimura M, Ohura T, Takahashi M, Kajiwara R, Ohura Jr. N. Mechanism leading to the development of pressure ulcers based on shear force and pressures during a bed operation: Influence of body types, body positions, and knee positions. *Wound Repair and Regeneration*. 2009;17(6). doi:10.1111/j.1524-475X.2009.00540.x

19. Wu Y, van der Schaft DWJ, Baaijens FP, Oomens CWJ. Cell death induced by mechanical compression on engineered muscle results from a gradual physiological mechanism. *Journal of Biomechanics*. 2016;49(7). doi:10.1016/j.jbiomech.2016.02.028

20. Jagannathan NS, Tucker-Kellogg L. Membrane permeability during pressure ulcer formation: A computational model of dynamic competition between cytoskeletal damage and repair. *Journal of Biomechanics*. 2016;49(8). doi:10.1016/j.jbiomech.2015.12.022

21. Oomens CWJ, Bressers OFJT, Bosboom EMH, Bouten CVC, Bader DL. Can Loaded Interface Characteristics Influence Strain Distributions in Muscle Adjacent to Bony Prominences? *Computer Methods in Biomechanics and Biomedical Engineering*. 2003;6(3):171-180.

22. Gefen A, Alves P, Ciprandi G, et al. Device-related pressure ulcers: SECURE prevention. *Journal of Wound Care*. 2020;29(Sup2a). doi:10.12968/jowc.2020.29.Sup2a.S1

23. Reichel SM. SHEARING FORCE AS A FACTOR IN DECUBITUS ULCERS IN PARAPLEGICS. *Journal of the American Medical Association*. 1958;166(7). doi:10.1001/jama.1958.62990070004010a

24. Bader DL, Worsley PR, Gefen A. Bioengineering considerations in the prevention of medical device-related pressure ulcers. *Clinical Biomechanics*. 2019;67. doi:10.1016/j.clinbiomech.2019.04.018

25. Manorama A, Meyer R, Wiseman R, Bush TR. Quantifying the effects of external shear loads on arterial and venous blood flow: Implications for pressure ulcer development. *Clinical Biomechanics*. 2013;28(5). doi:10.1016/j.clinbiomech.2013.04.001

26. Bishopp A, Oakes A, Antoine-Pitterson P, Chakraborty B, Cormer D, Mukherjee R. The preventative effect of hydrocolloid dressings on Nasal bridge pressure ulceration in acute non- invasive ventilation. *Ulster Med J*. 2019;88(1):17-20.

27. Moore ZE, Webster J. Dressings and topical agents for preventing pressure ulcers. *Cochrane Database of Systematic Reviews*. 2018;12(12). doi:10.1002/14651858.CD009362.pub3

28. Kantor J. Behavioral considerations and impact on personal protective equipment use: Early lessons from the coronavirus (COVID-19) pandemic. *Journal of the American Academy of Dermatology*. 2020;82(5). doi:10.1016/j.jaad.2020.03.013

29. Lei Z, Yang J (James), Zhuang Z. Headform and N95 Filtering Facepiece Respirator Interaction: Contact Pressure Simulation and Validation. *Journal of Occupational and Environmental Hygiene*. 2012;9(1):46-58. doi:10.1080/15459624.2011.635130

30. Lei Z, Yang J, Zhuang Z. Contact Pressure Study of N95 Filtering Face-piece Respirators Using Finite Element Method. *Computer-Aided Design and Applications*. 2010;7(6):847-861. doi:10.3722/cadaps.2010.847-861

31. Lei Z, Ji X, Yang J, Zhuang Z, Rottach D. Simulated Effects of Head Movement on Contact Pressures between Headforms and N95 Filtering Facepiece Respirators Part 2: Simulation. *The Annals of Occupational Hygiene*. Published online September 3, 2014. doi:10.1093/annhyg/meu064

32. Rausch MK, Karniadakis GE, Humphrey JD. Modeling Soft Tissue Damage and Failure Using a Combined Particle/Continuum Approach. *Biomechanics and Modeling in Mechanobiology*. 2017;16(1). doi:10.1007/s10237-016-0814-1

33. Oomens CWJ, Bader DL, Loerakker S, Baaijens F. Pressure Induced Deep Tissue Injury Explained. *Annals of Biomedical Engineering*. 2015;43(2). doi:10.1007/s10439-014-1202-6

34. Hertz H. Ueber die Berührung fester elastischer Körper. *Journal für die reine und angewandte Mathematik (Crelles Journal)*. 1882;1882(92). doi:10.1515/crll.1882.92.156

35. Xing M, Pan N, Zhong W, Maibach H. Skin friction blistering: computer model. *Skin Research and Technology*. 2007;13(3). doi:10.1111/j.1600-0846.2007.00230.x

36. Polliack AA, Scheinberg S. A New Technology for Reducing Shear and Friction Forces on the Skin: Implications for Blister Care in the Wilderness Setting. *Wilderness & Environmental Medicine*. 2006;17(2). doi:10.1580/PR30-05.1

37. Aumailley M, Rousselle P. Laminins of the dermo–epidermal junction. *Matrix Biology*. 1999;18(1). doi:10.1016/S0945-053X(98)00004-3

38. Hatje LK, Richter C, Blume-Peytavi U, Kottner J. Blistering time as a parameter for the strength of dermoepidermal adhesion: a systematic review and meta-analysis. *British Journal of Dermatology*. 2015;172(2). doi:10.1111/bjd.13298

39. Masen MA, Chung A, Dawczyk JU, et al. Evaluating lubricant performance to reduce COVID-19 PPE-related skin injury. *PLOS ONE*. 2020;15(9). doi:10.1371/journal.pone.0239363

40. Yap KK, Murali M, Tan Z, Zhou X, Li L, Masen M. Wax-Oil Lubricants to Reduce the Shear Between Skin and PPE. *Article submitted to Scientific Reports*.

41. van Kuilenburg J, Masen MA, van der Heide E. The role of the skin microrelief in the contact behaviour of human skin: Contact between the human finger and regular surface textures. *Tribology International*. 2013;65:81-90. doi:10.1016/j.triboint.2012.11.024

42. Klaassen M, de Vries EG, Masen MA. Friction in the contact between skin and soft counter material: Effects of hardness and surface finish. *Journal of the Mechanical Behaviour of Biomedical Materials*. 2019;92:137-143. doi:10.1016/j.jmbbm.2019.01.006

43. Aly R, Shirley C, Cunico B, Maibach HI. Effect of Prolonged Occlusion on the Microbial Flora, pH, Carbon Dioxide and Transepidermal Water Loss on Human Skin. *Journal of Investigative Dermatology*. 1978;71(6). doi:10.1111/1523-1747.ep12556778

44. Geerligs M, Oomens C, Ackermans P, Baaijens F, Peters G. Linear shear response of the upper skin layers. *Biorheology*. 48(3-4):229-245.

45. Klaassen M, Schipper DJ, Masen MA. Influence of the relative humidity and the temperature on the in-vivo friction behaviour of human skin. *Biotribology*. 2016;6. doi:10.1016/j.biotri.2016.03.003

46. Gerhardt L-C, Strässle V, Lenz A, Spencer ND, Derler S. Influence of epidermal hydration on the friction of human skin against textiles. *Journal of The Royal Society Interface*. 2008;5(28). doi:10.1098/rsif.2008.0034

47. Kleesz P, Darlenski R, Fluhr JW. Full-Body Skin Mapping for Six Biophysical Parameters: Baseline Values at 16 Anatomical Sites in 125 Human Subjects. *Skin Pharmacology and Physiology*. 2012;25(1). doi:10.1159/000330721

48. Tang W, Zhou Y, Zhu H, Yang H. The effect of surface texturing on reducing the friction and wear of steel under lubricated sliding contact. *Applied Surface Science*. 2013;273:199-204. doi:10.1016/j.apsusc.2013.02.013

49. Zhang M, Mak AFT. In vivo friction properties of human skin. *Prosthetics & Orthotics International*. 1999;23(2). doi:10.3109/03093649909071625

50. Granta Design Limited. CES EduPack software. Published online 2020.

51. Seo NJ, Armstrong TJ, Drinkaus P. A comparison of two methods of measuring static coefficient of friction at low normal forces: a pilot study. *Ergonomics*. 2009;52(1). doi:10.1080/00140130802238622

52. Luboz V, Promayon E, Payan Y. Linear Elastic Properties of the Facial Soft Tissues Using an Aspiration Device: Towards Patient Specific Characterization. *Annals of Biomedical Engineering*. 2014;42(11). doi:10.1007/s10439-014-1098-1

53. Farkas LG, Katic MJ, Forrest CR. International Anthropometric Study of Facial Morphology in Various Ethnic Groups/Races. *Journal of Craniofacial Surgery*. 2005;16(4). doi:10.1097/01.scs.0000171847.58031.9e

54. Dong Y, Huang L, Feng Z, Bai S, Wu G, Zhao Y. Influence of sex and body mass index on facial soft tissue thickness measurements of the northern Chinese adult population. *Forensic Science International*. 2012;222(1-3). doi:10.1016/j.forsciint.2012.06.004

55. Ascott A, Crowest P, de Sausmarez E, Khan M, Chakladar A. Respiratory personal protective equipment for healthcare workers: impact of sex differences on respirator fit test results. *British Journal of Anaesthesia*. 2021;126(1). doi:10.1016/j.bja.2020.10.016

56. Xu M, Yang J. Contact Pressure Sensitivity Analysis in N95 Filtering Facepiece Respirator With Strap Location, Friction, and Headform Material Property. In: *Volume 1A: 35th Computers and Information in Engineering Conference*. American Society of Mechanical Engineers; 2015. doi:10.1115/DETC2015-46465

57. Simulated Effects of Head Movement on Contact Pressures Between Headforms and N95 Filtering Facepiece Respirators-Part 1: Headform Model and Validation. *The Annals of Occupational Hygiene*. Published online September 3, 2014. doi:10.1093/annhyg/meu051

58. van Kuilenburg J, Masen MA, van der Heide E. Contact modelling of human skin: What value to use for the modulus of elasticity? *Proceedings of the Institution of Mechanical Engineers, Part J: Journal of Engineering Tribology*. 2013;227(4). doi:10.1177/1350650112463307

59. Xu M, Yang J. Human Facial Soft Tissue Thickness and Mechanical Properties: A Literature Review. In: *Volume 1A: 35th Computers and Information in Engineering Conference*. American Society of Mechanical Engineers; 2015. doi:10.1115/DETC2015-46363

60. Chopra K, Calva D, Sosin M, et al. A Comprehensive Examination of Topographic Thickness of Skin in the Human Face. *Aesthetic Surgery Journal*. 2015;35(8). doi:10.1093/asj/sjv079

61. Maiti R, Duan M, Danby SG, Lewis R, Matcher SJ, Carré MJ. Morphological parametric mapping of 21 skin sites throughout the body using optical coherence tomography. *Journal of the Mechanical Behavior of Biomedical Materials*. 2020;102. doi:10.1016/j.jmbbm.2019.103501

62. Hendriks CP, Franklin SE. Influence of Surface Roughness, Material and Climate Conditions on the Friction of Human Skin. *Tribology Letters*. 2010;37(2). doi:10.1007/s11249-009-9530-7

63. Adams MJ, Briscoe BJ, Johnson SA. Friction and lubrication of human skin. *Tribology Letters*. 2007;26(3). doi:10.1007/s11249-007-9206-0

Figures

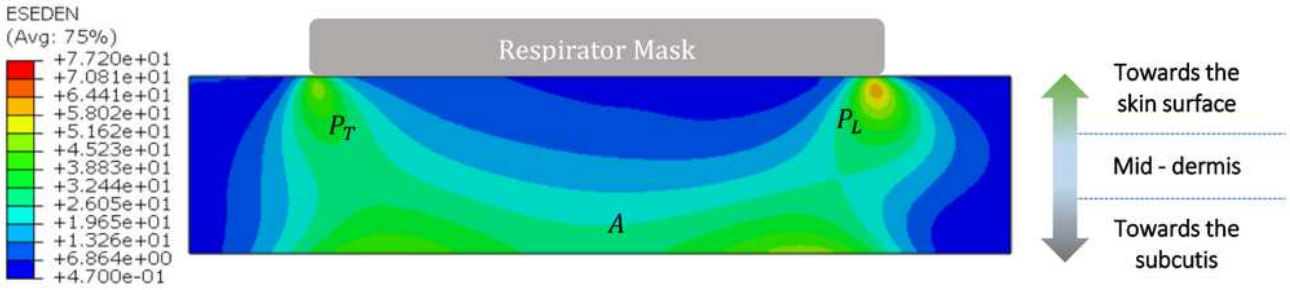

(a) The reference situation (E = 100 kPa, ν = 0.4, L_c = 4 mm and μ = 0.5) shows a SED distribution that has two characteristic peaks in the upper dermis near the skin surface, P_L at the leading edge and P_T at the trailing edge of the contact with the PPE. Due to the friction in the PPE-skin interface, the distribution is asymmetrical and the value for the SED at the leading edge is elevated compared to the trailing edge. The typical SED distribution also includes a large area of elevated SED deeper within the dermis, marked A, towards the subcutis.

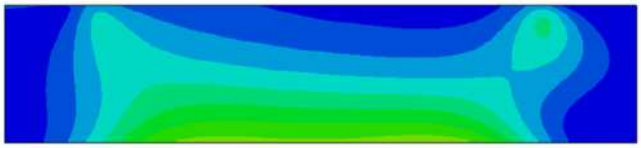

(b) When applying a compliant material (E = 5kPa) the SED reduces in the two peaks P_L and P_T, whilst deeper into the tissue, the SED appears elevated as marked by the larger area A.

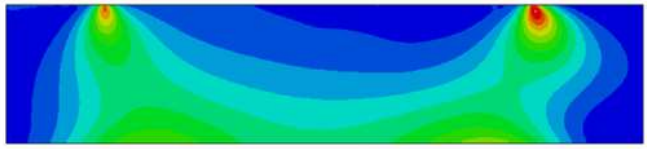

(c) For a stiff mask material (E = 5MPa), the SED at P_L and P_T is strongly increase, whilst being reduced towards the central deeper tissue A.

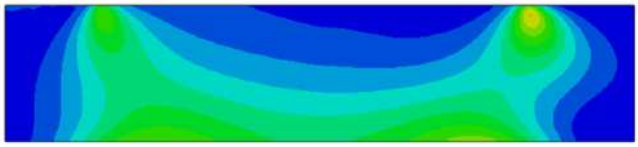

(d) A material with a Poisson's ratio ν= 0.1 results in a decreased SED in the upper dermisP_L, P_T with no substantial effect on the SED in the lower dermis A.

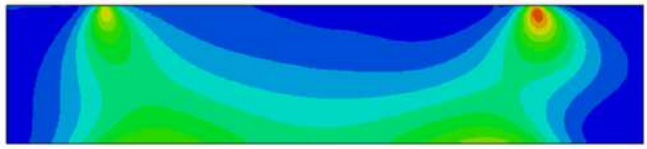

(e) A near incompressible material ν= 0.49 elevates SED at P_L and P_T. Whilst there is little effect on the SED in the lower dermis A, the SED in the region between P_L and A is elevated.

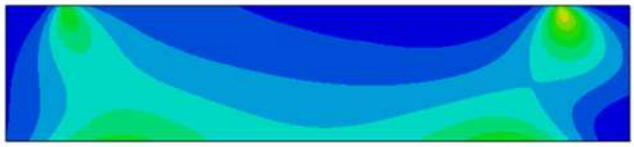

(f) When the load is distributed over a larger area of contact between the mask and the skin, in this case a contact length of 4.8 mm, the SED is distributed over a larger area and the SED is reduced throughout the skin.

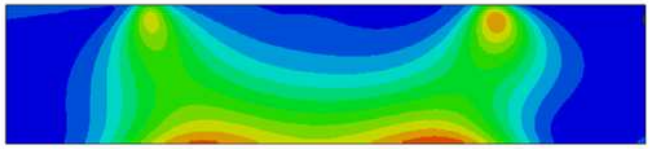

(g) For a smaller contact area, in this case a contact length of 3 mm, the SED is strongly increased, particularly deeper into the skin at region A. Compared to the reference situation, the increase at P_L and P_T is marginal.

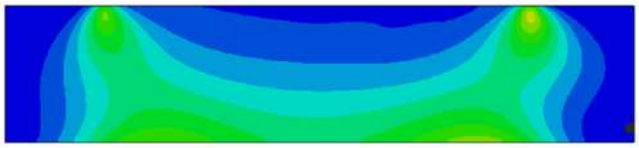

(h) Reducing the coefficient of friction (μ = 0.2) in the interface, reduces the SED values near the surface, particularly in P_L. The SED values between P_L and A increase slightly. No significant changes were observed for region A.

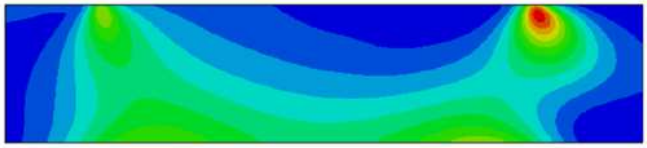

(i) Increasing the coefficient of friction (μ = 0.8) in the interface strongly increase SED at P_L. The effect deeper in the surface, in region A appears negligible. A minor decrease of SED values can be observed between P_L and A indicating a sharper, more isolated peak in P_L.

Figure 1

Distribution of the SED in the dermis as a result of using PPE. Red indicates an elevated value. Distribution displayed overlayed over the undeformed tissue.

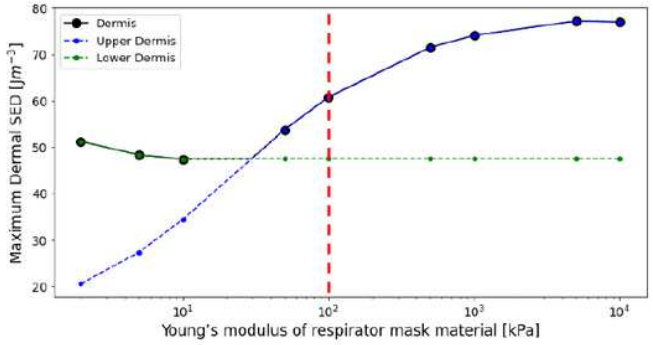

(a) *With all other parameters held constant, stiffer mask materials result in the maximum dermal SED to be located in the upper dermis (blue). Below E ≈ 30 kPa the maximum SED occurs in the lower dermis and its value increases with reducing mask stiffness.*

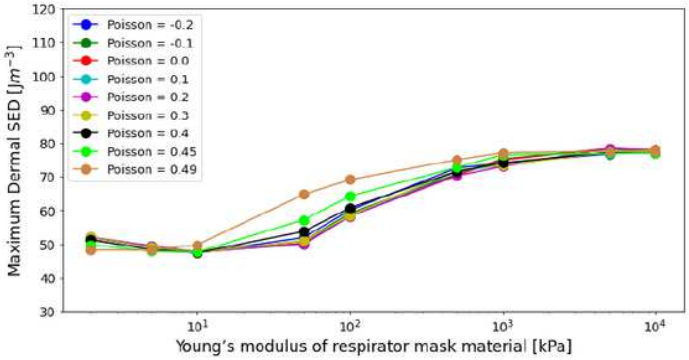

(b) *Nearly incompressible materials (v → 0.5) with intermediate levels of stiffness (10 kPa < E < 1000 kPa) result in increases in maximum SED.*

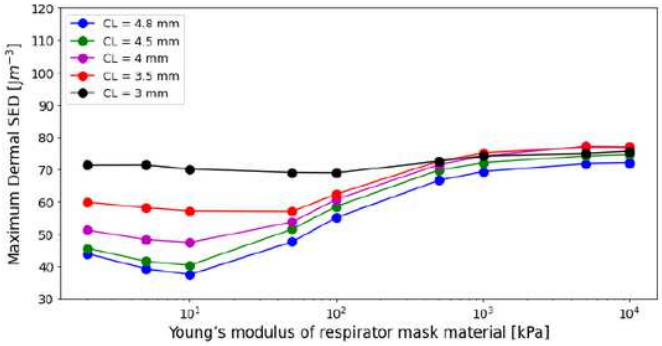

(c) *A larger contact area between the skin and mask results in lower maximum SED values in the dermis. This effect is particularly pronounced for softer materials.*

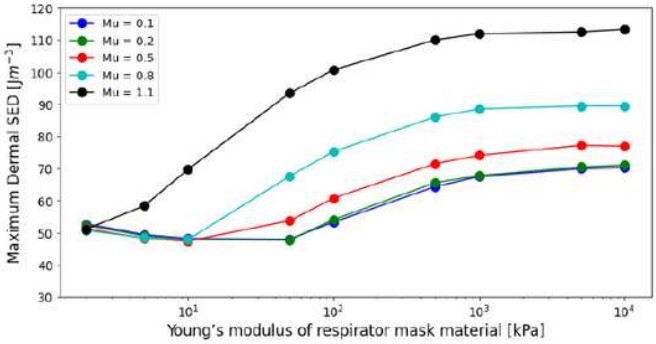

(d) *For mask material stiffnesses above 10 kPa an increased interfacial friction coefficient results in substantially higher SED values in the upper dermis, particularly at the leading edge of the contact, P_L.*

Figure 2

The effects of independently altering the mask properties on the maximum SED in the tissue. (a) Mask material stiffness, (b) Poisson's ratio, (b) area of contact, and (d) interfacial friction coefficient.

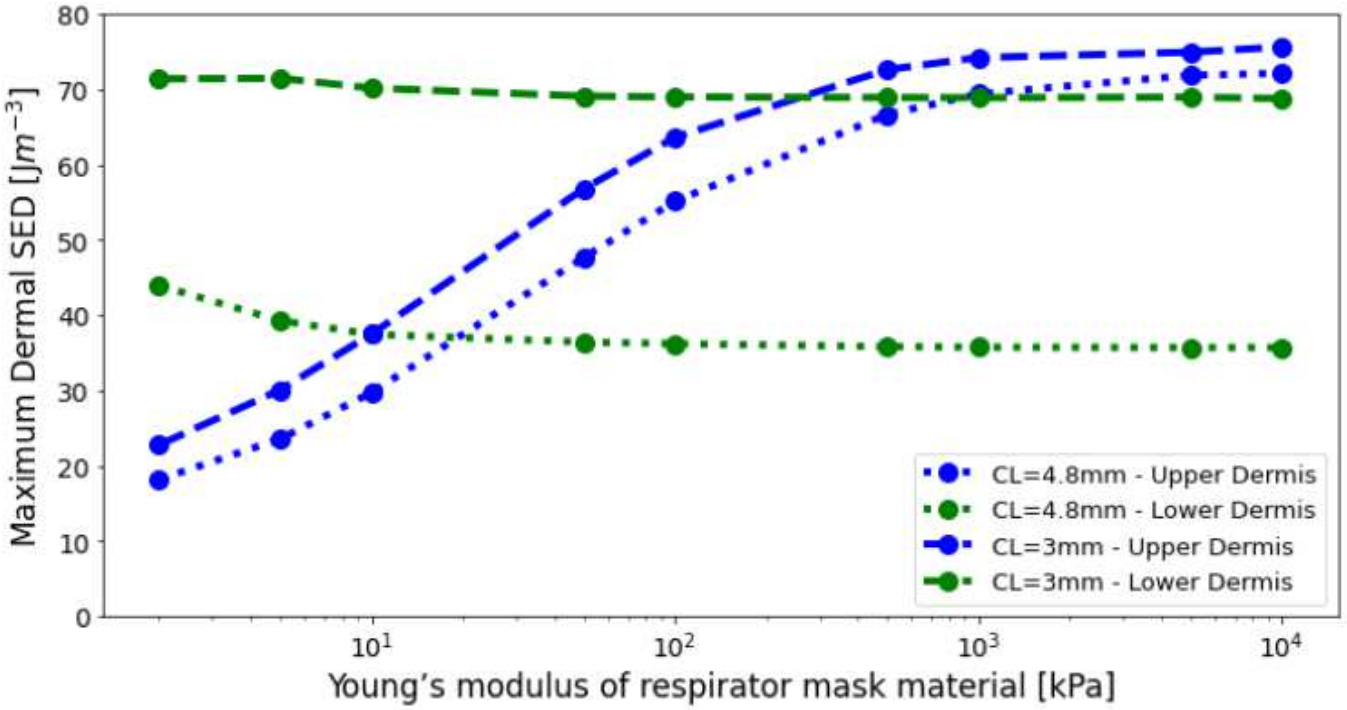

Figure 3

Evolution of SED in the tissue as a function of mask material modulus for contact lengths of 4.8 mm and 3 mm. Changes in contact length had a substantial effect on maximum SED in the lower dermis compared to the upper dermis.

Model/Parameter	E [kPa]	ν [-]	L_C [mm]	μ [-]
Silicone	210	0.49	4	0.6
Geometry altered	210	0.49	4.8	0.6
Interface altered	210	0.49	4	0.2
Materials altered	50	0.4	4	0.6
Improved PPE	50	0.4	4.8	0.2

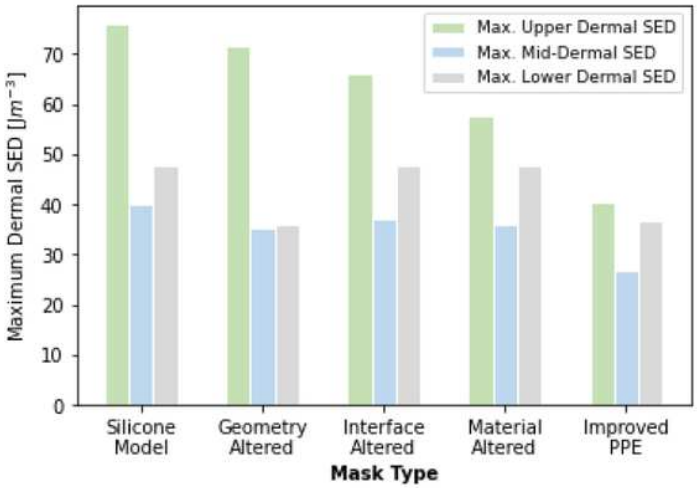

Figure 4

Table (left) showing different mask modifications compared to a silicone-based model. Graph (right) showing the SED in the upper (green), middle (blue) and lower dermis (grey) in response to the modifications.

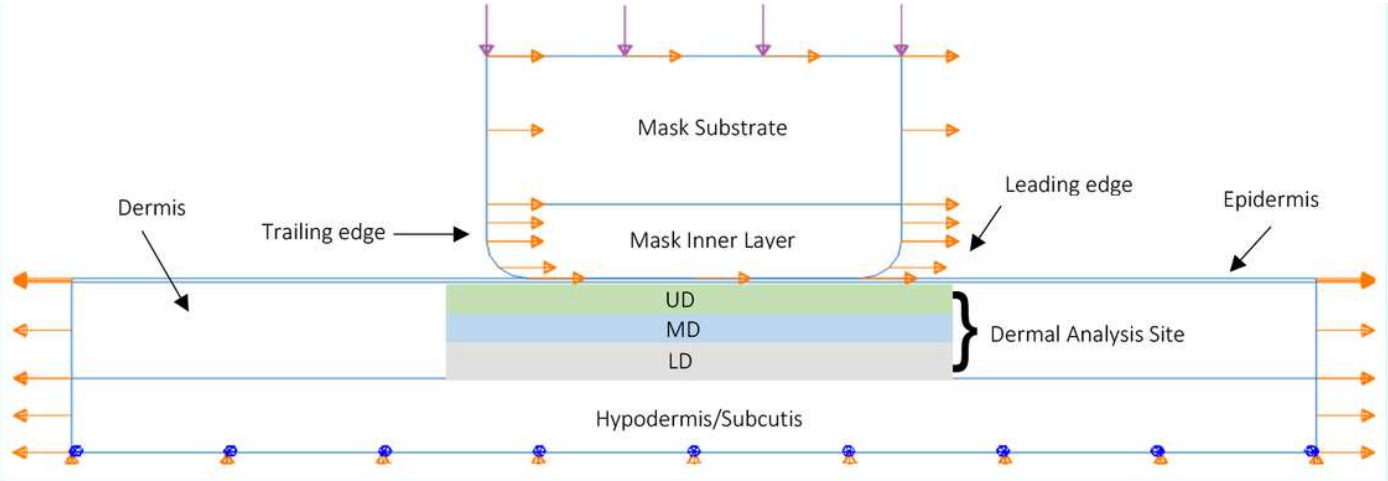

Figure 5

Schematic diagram detailing the compression and translation of a mask model against a skin model, in order to simulate PPE- Skin contact.